Supporting Information

for

Molecular industry of cage metal complexes for biological applications: pathways of the synthesis, X-ray structure of a series of new N_2-, S_2- and O_2-alicyclic iron(II) di- and tetrachloroclathrochelates

Genrikh E. Zelinskii [1], Alexander S. Belov [1], Irina G. Belaya [1], Anna V. Vologzhanina [1], Valentin V. Novikov [1], Oleg A. Varzatskii [2], Yan Z. Voloshin [1,3,*]

[1] *Nesmeyanov Institute of Organoelement Compounds of the Russian Academy of Sciences; 119991 Moscow, Russia; e-mail: voloshin@ineos.ac.ru*

[2] *Vernadskii Institute of General and Inorganic Chemistry NASU, 03680, Kiev, Ukraine*

[3] *Kurnakov Institute of General and Inorganic Chemistry of the Russian Academy of Sciences, 119991, Moscow, Russia*

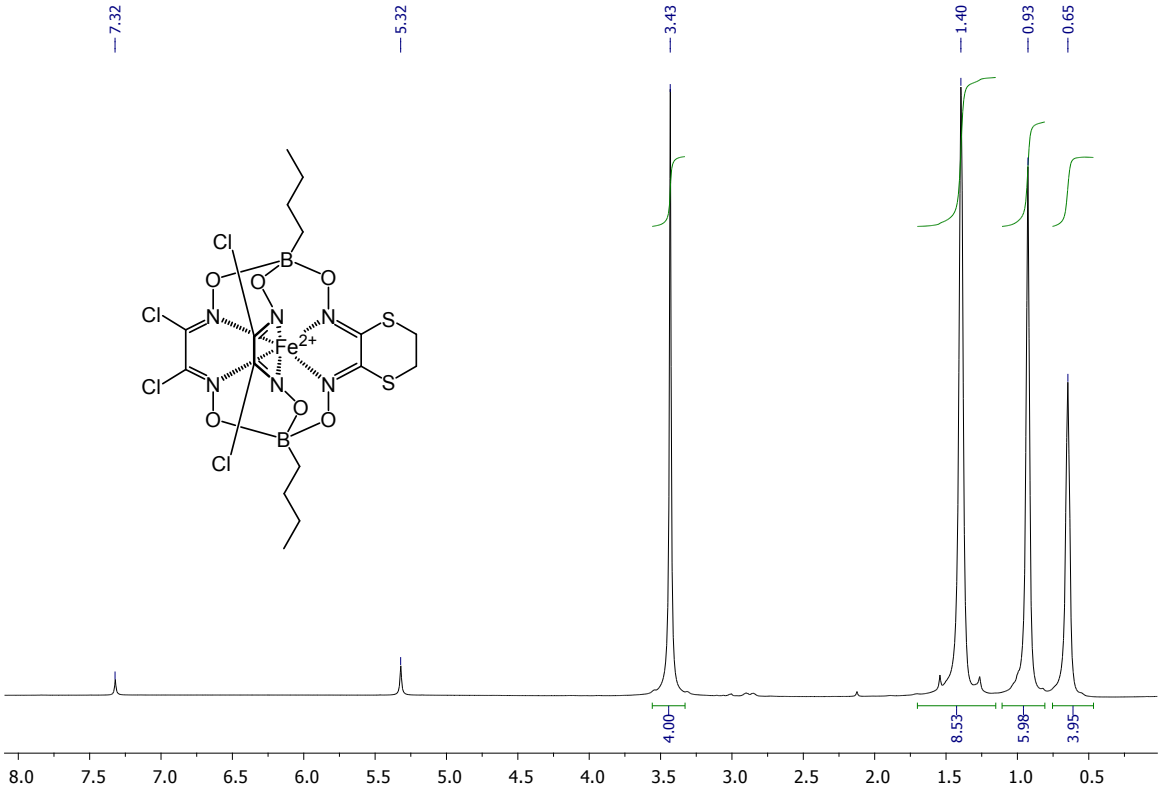

Figure S1. ^{1}H NMR spectrum for the CD_2Cl_2 solution of the clathrochelate Fe(S_2-Nx)(Cl_2Gm)$_2$(B*n*-C_4H_9)$_2$ (**1**).

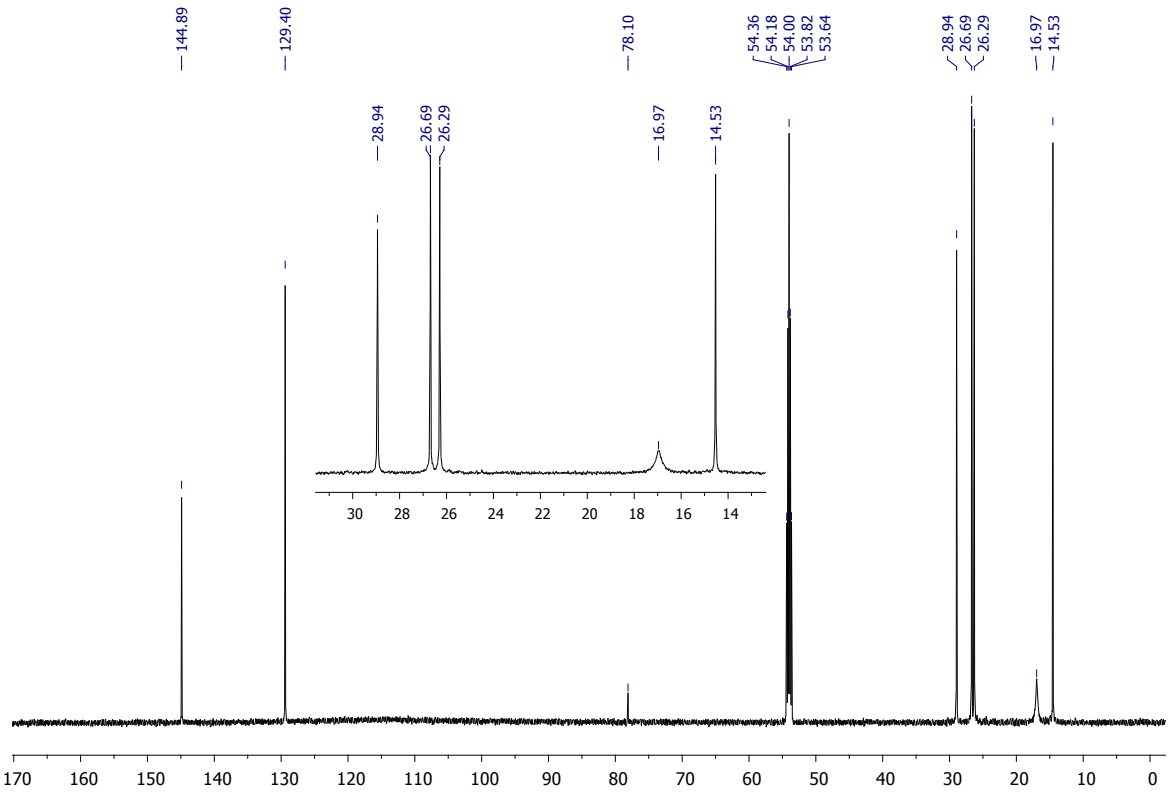

Figure S2. $^{13}C\{^{1}H\}$ NMR spectrum for the CD_2Cl_2 solution of the clathrochelate $Fe(S_2\text{-Nx})(Cl_2Gm)_2(B\textit{n}\text{-}C_4H_9)_2$ (**1**).

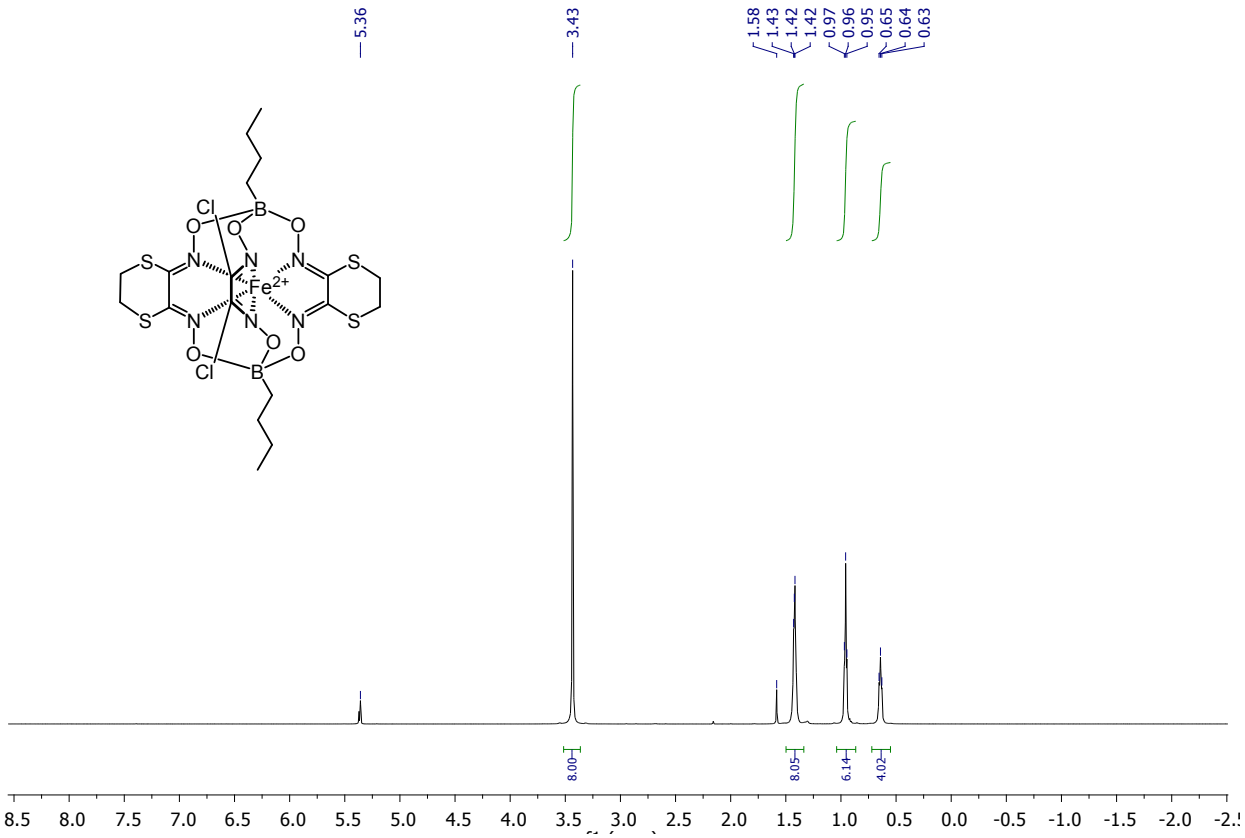

Figure S3. ^{1}H NMR spectrum for the CD_2Cl_2 solution of the clathrochelate Fe(S_2-Nx)$_2$(Cl_2Gm)(B*n*-C_4H_9)$_2$ (**2**).

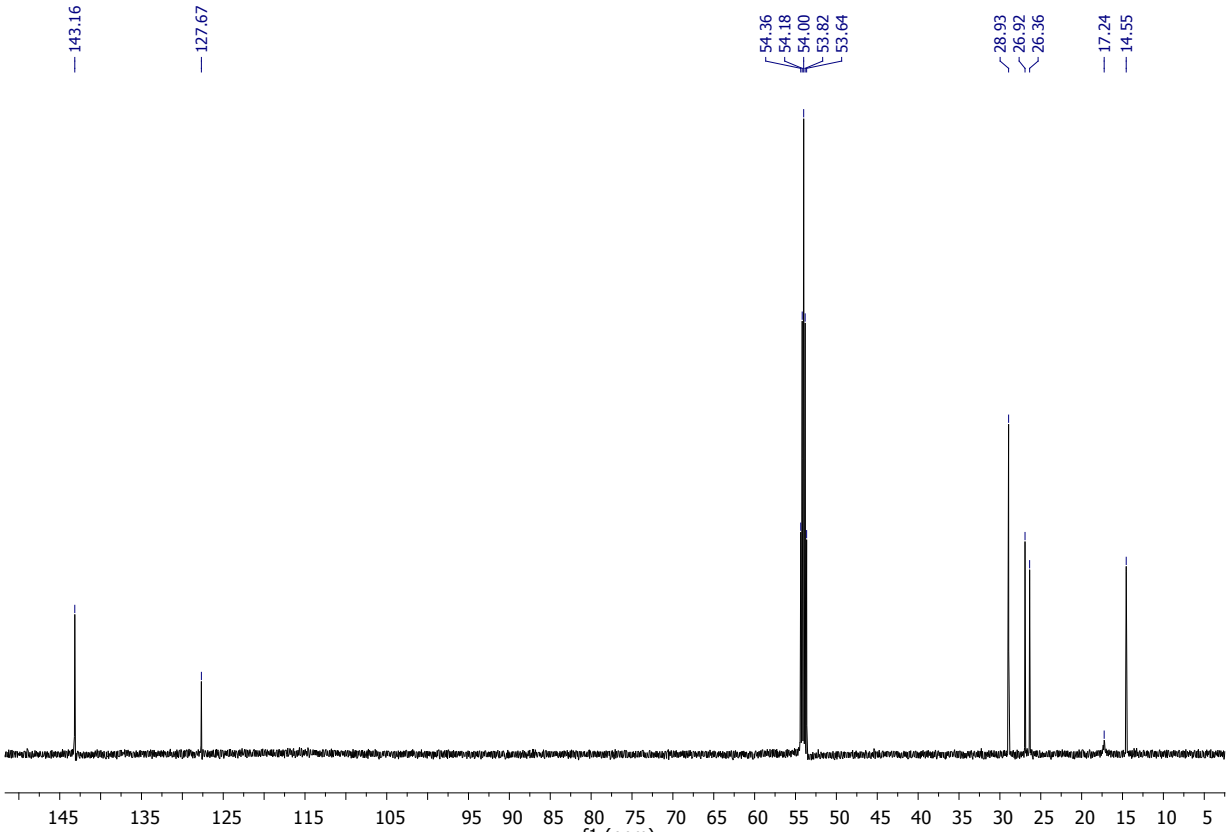

δ^{13}_{C} (ppm)

Figure S4. $^{13}C\{^{1}H\}$ NMR spectrum for the CD_2Cl_2 solution of the clathrochelate $Fe(S_2\text{-}Nx)_2(Cl_2Gm)(B\textit{n}\text{-}C_4H_9)_2$ (**2**).

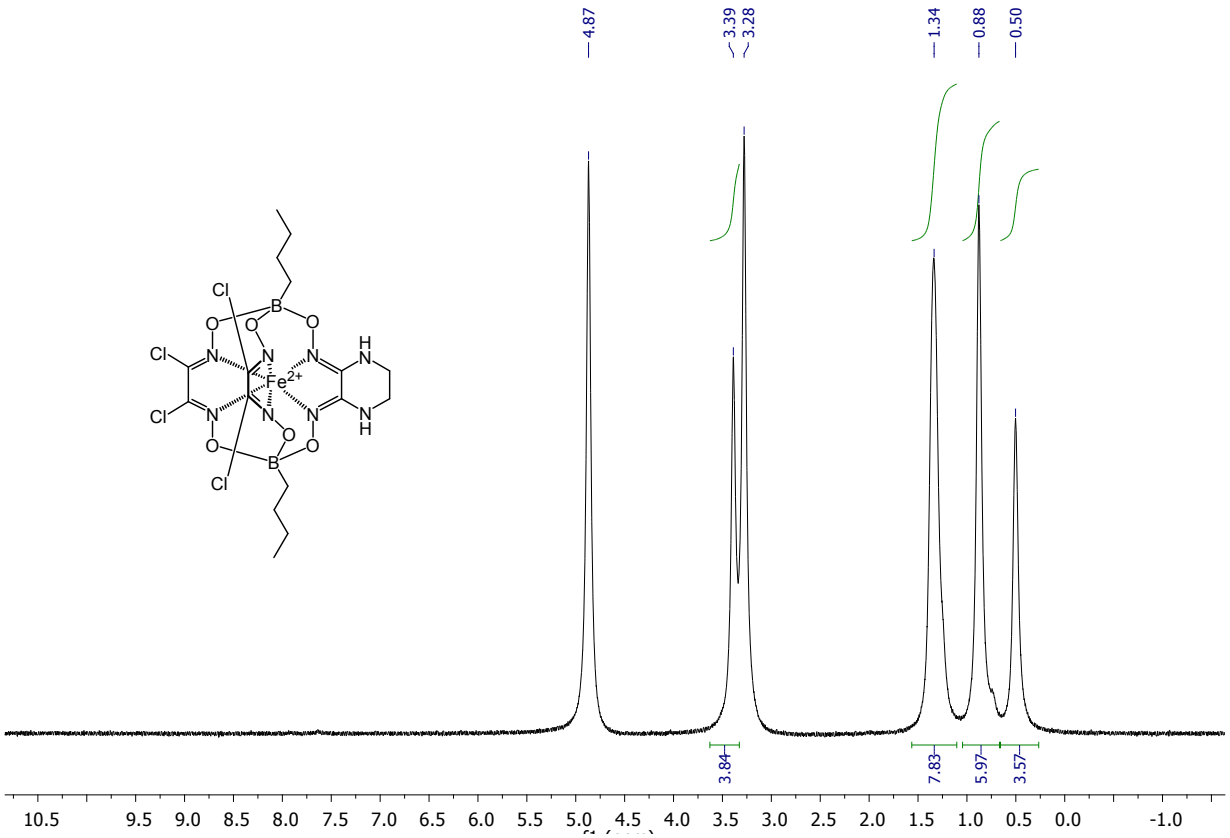

Figure S5. ^{1}H NMR spectrum for the CD_3OD solution of the clathrochelate Fe(N_2-Nx)(Cl_2Gm)$_2$(B*n*-C_4H_9)$_2$ (**3**).

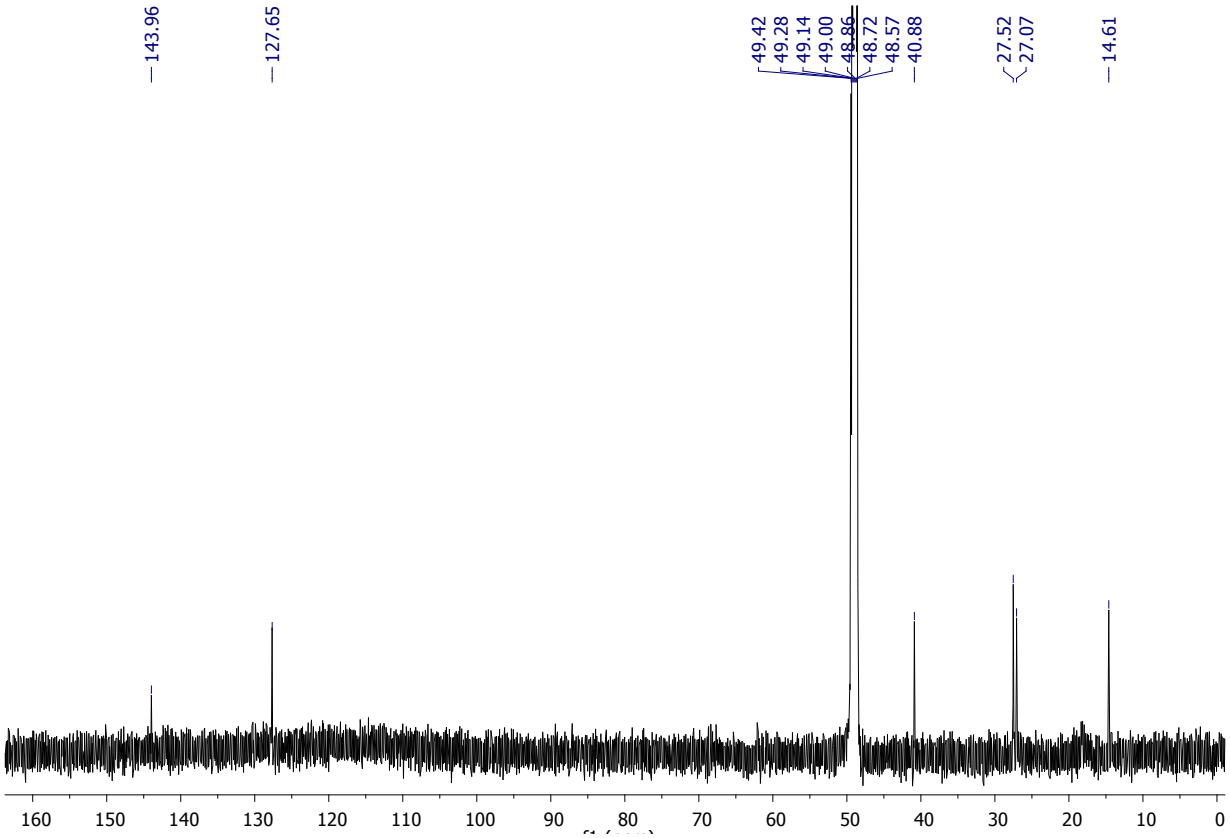

Figure S6. $^{13}C\{^{1}H\}$ NMR spectrum for the CD_3OD solution of the clathrochelate $Fe(N_2\text{-}Nx)(Cl_2Gm)_2(B\textit{n}\text{-}C_4H_9)_2$ (**3**).

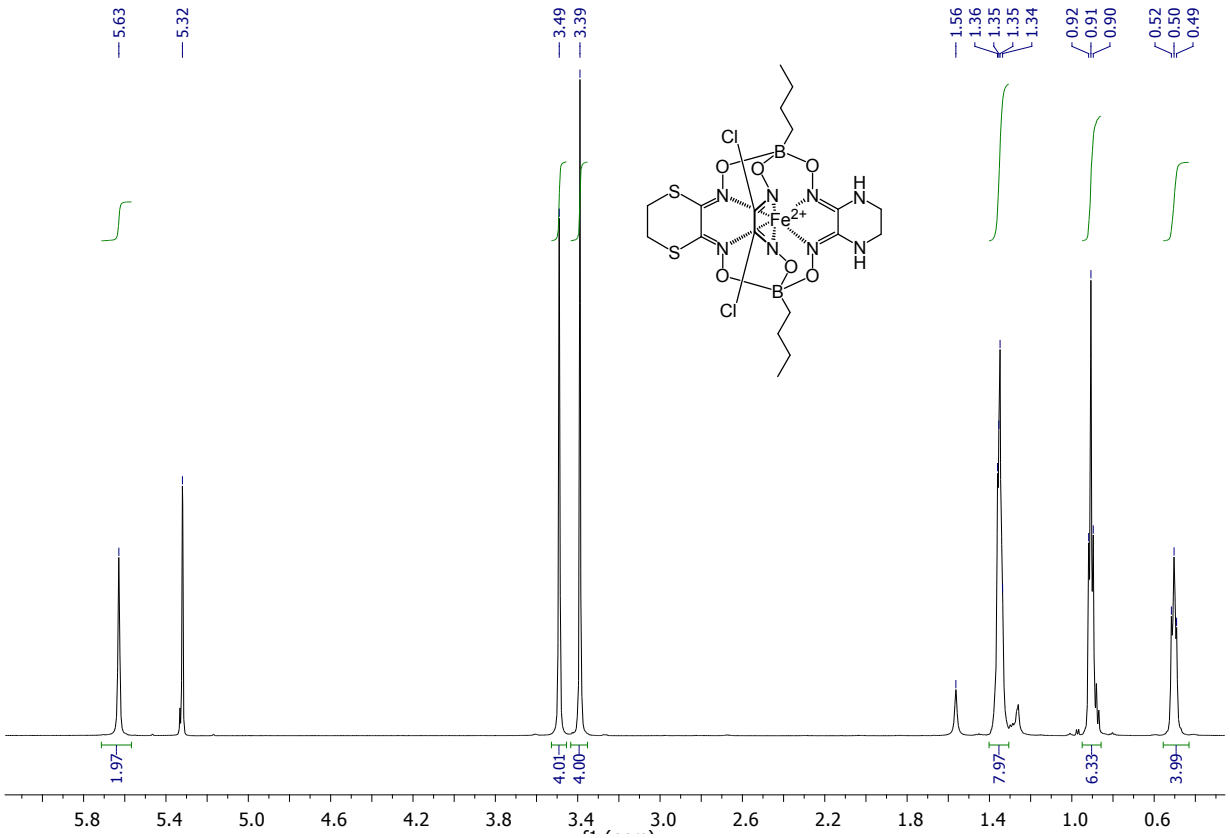

Figure S7. ^{1}H NMR spectrum for the CD_2Cl_2 solution of the clathrochelate Fe(N_2-Nx)(S_2-Nx)(Cl_2Gm)(B*n*-C_4H_9)$_2$ (**4**).

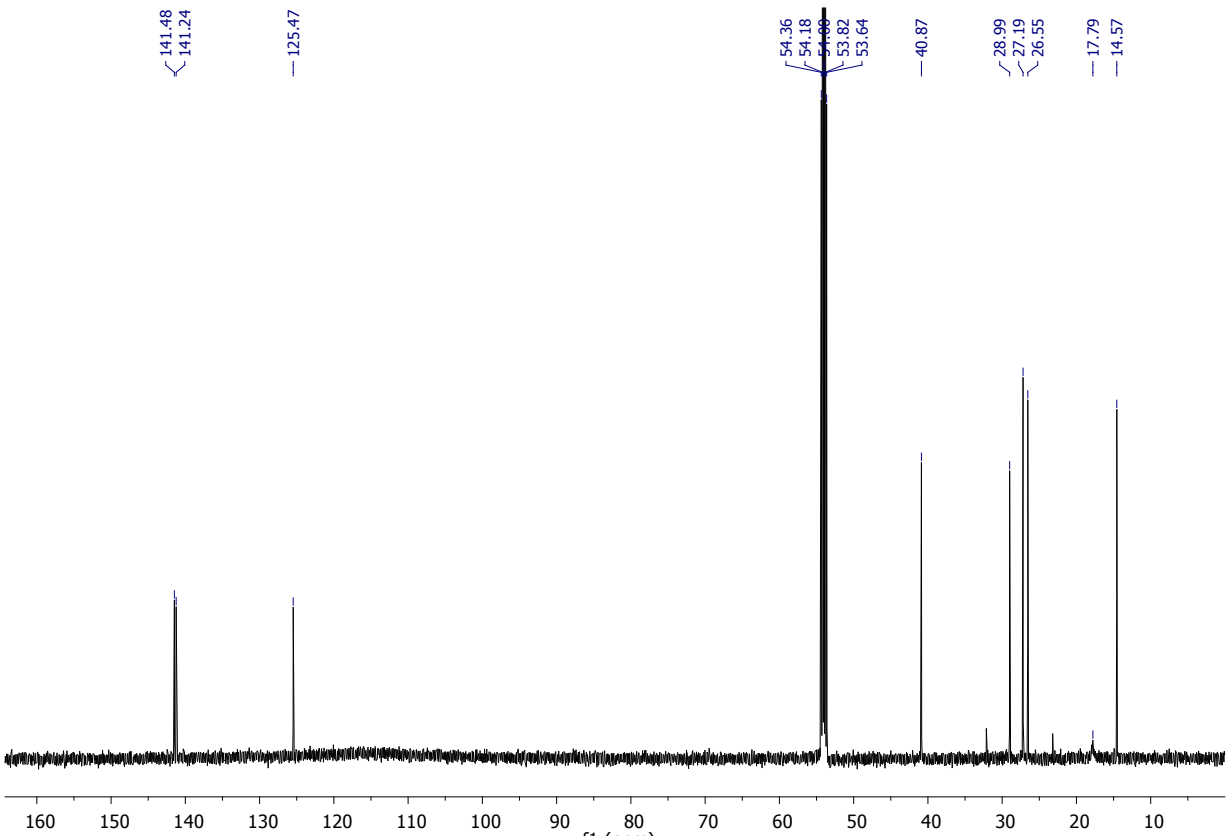

$\delta^{13}C$ (ppm)

Figure S8. $^{13}C\{^{1}H\}$ NMR spectrum for the CD_2Cl_2 solution of the clathrochelate Fe(*N*$_2$-Nx)(*S*$_2$-Nx)(Cl_2Gm)(B*n*-C_4H_9)$_2$ (**4**).

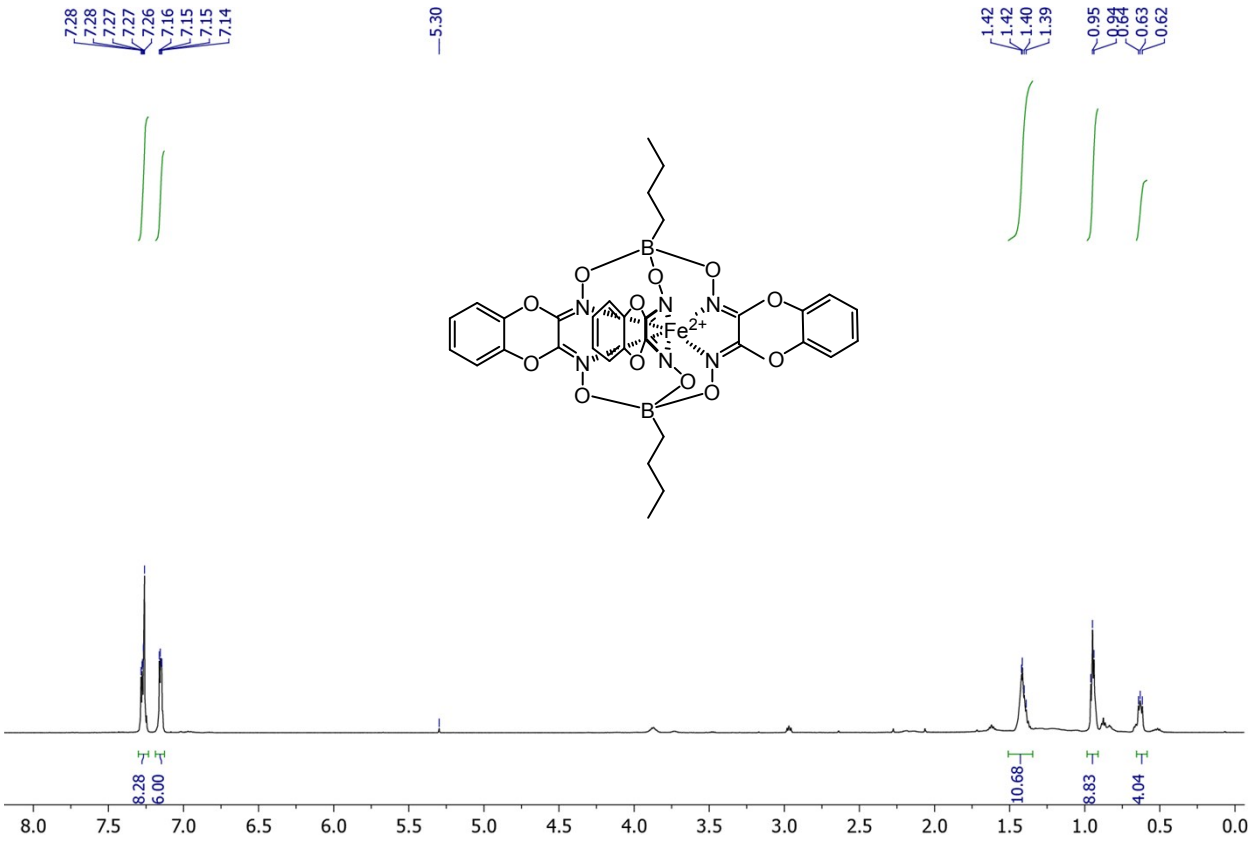

$\delta_{^1H}$ (ppm)

Figure S9. ^{1}H NMR spectrum for the $CDCl_3$ solution of the clathrochelate $Fe(PrchGm)_3(B\textit{n}\text{-}C_4H_9)_2$ (**5**).

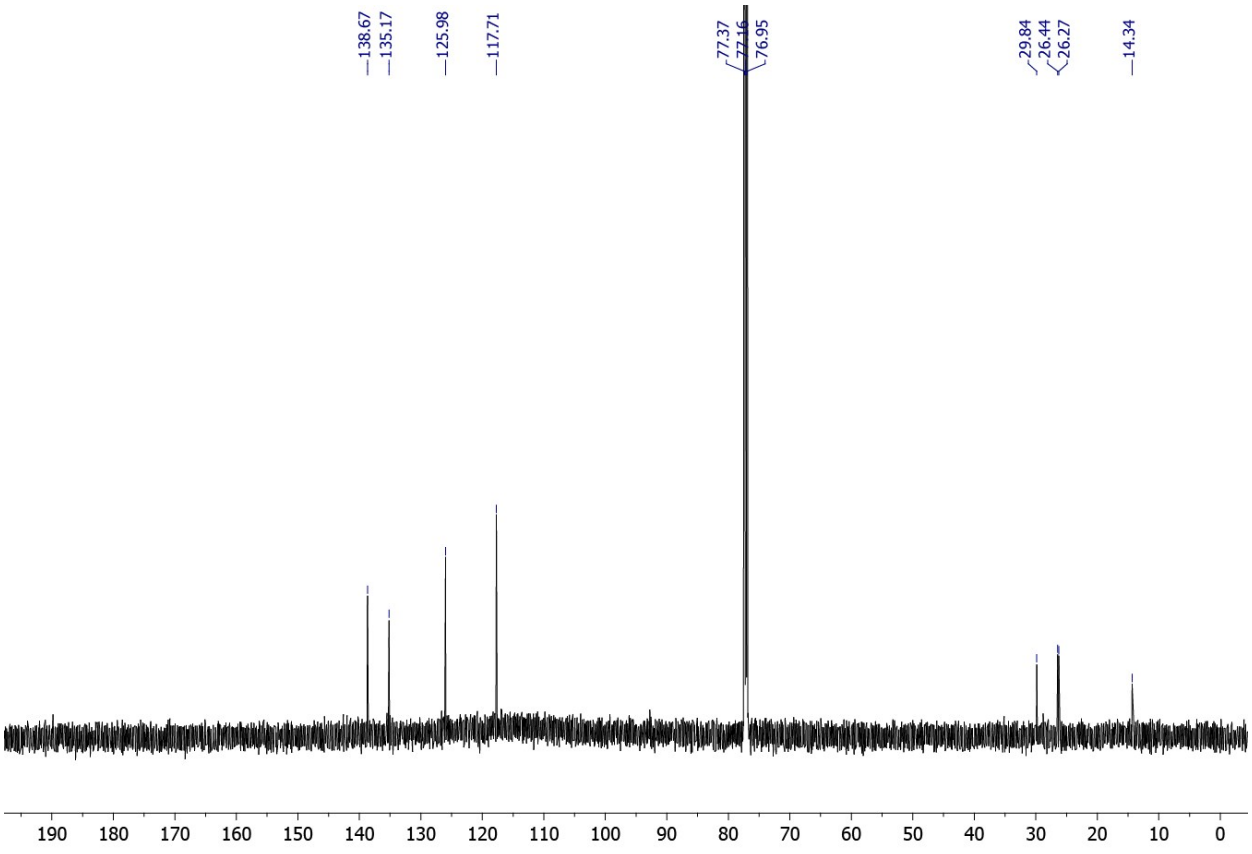

Figure S10. $^{13}C\{^{1}H\}$ NMR spectrum for the $CDCl_3$ solution of the clathrochelate $Fe(PrchGm)_3(B\textit{n}\text{-}C_4H_9)_2$ (**5**).

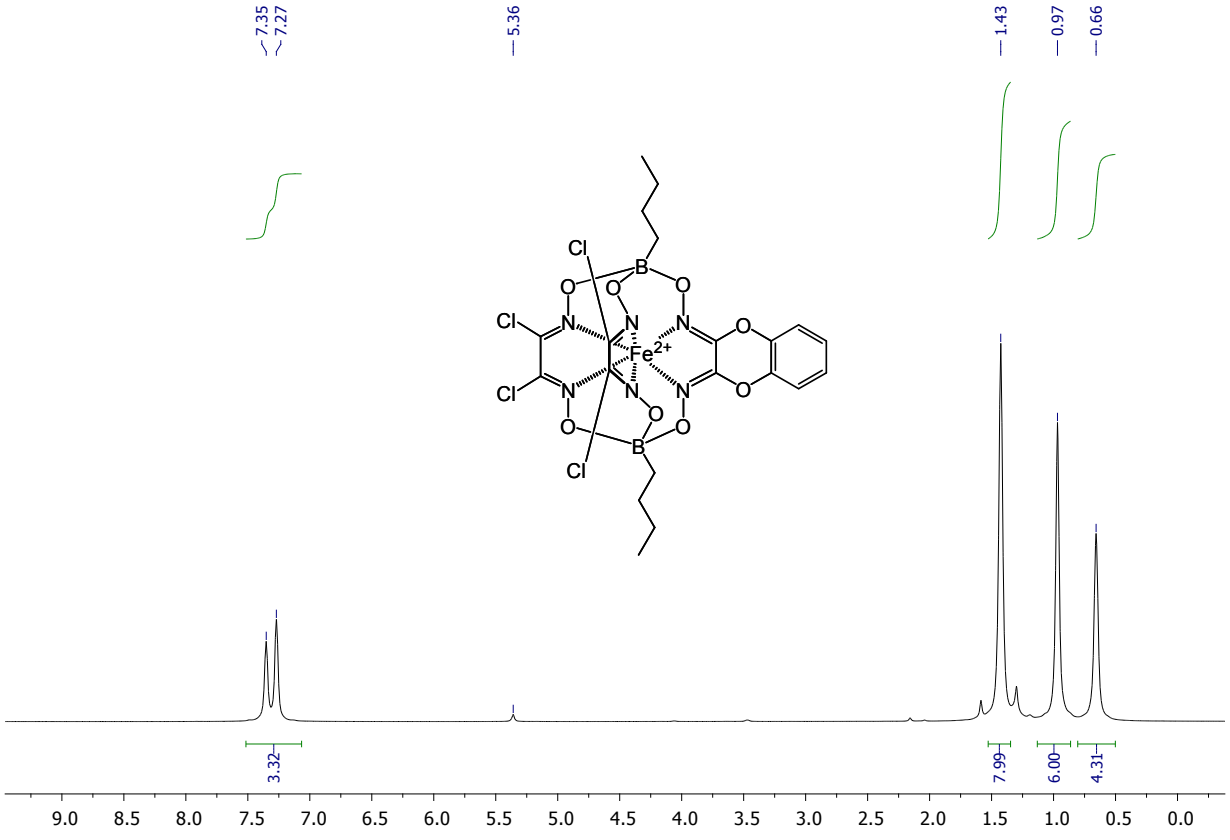

Figure S11. ^{1}H NMR spectrum for the CD_2Cl_2 solution of the clathrochelate $Fe(Cl_2Gm)_2(PrchGm)(B\textit{n}\text{-}C_4H_9)_2$ (**6**).

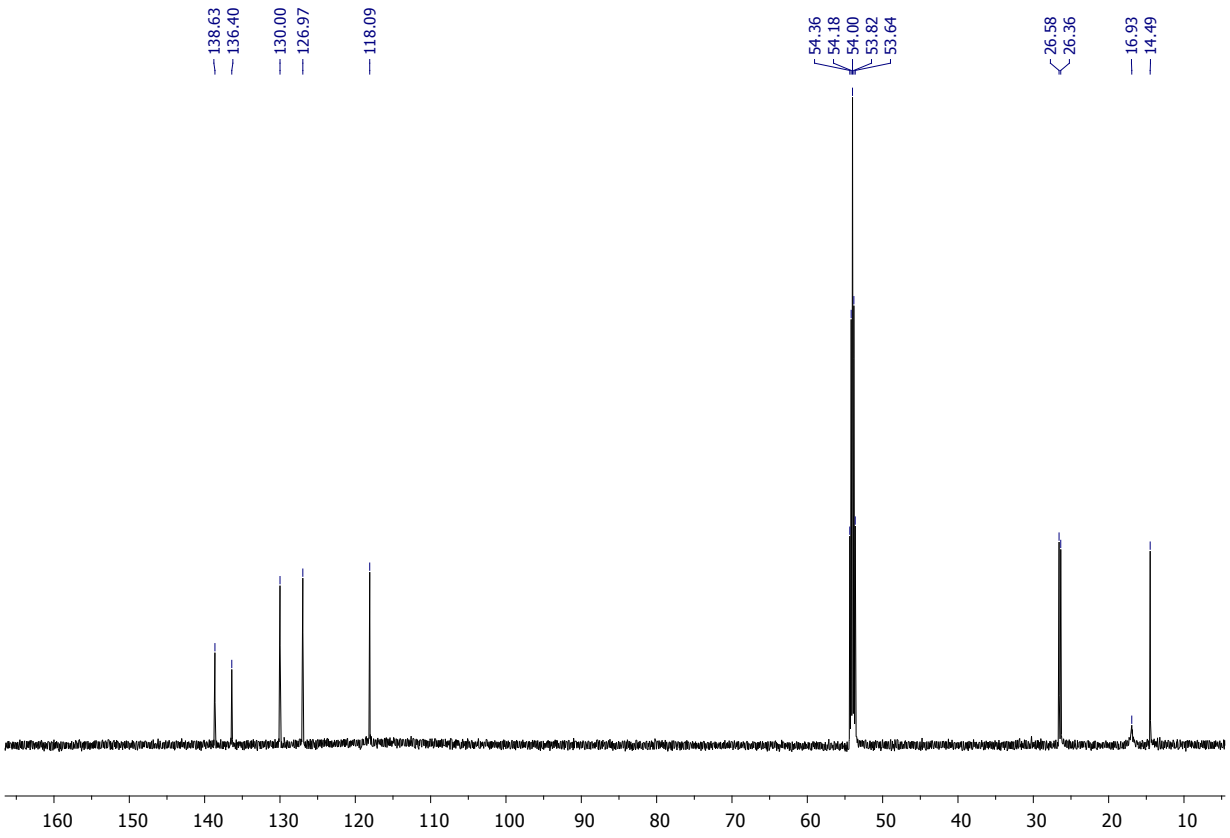

Figure S12. $^{13}C\{^{1}H\}$ NMR spectrum for the CD_2Cl_2 solution of the clathrochelate $Fe(Cl_2Gm)_2(PrchGm)(B\textit{n}\text{-}C_4H_9)_2$ (**6**).

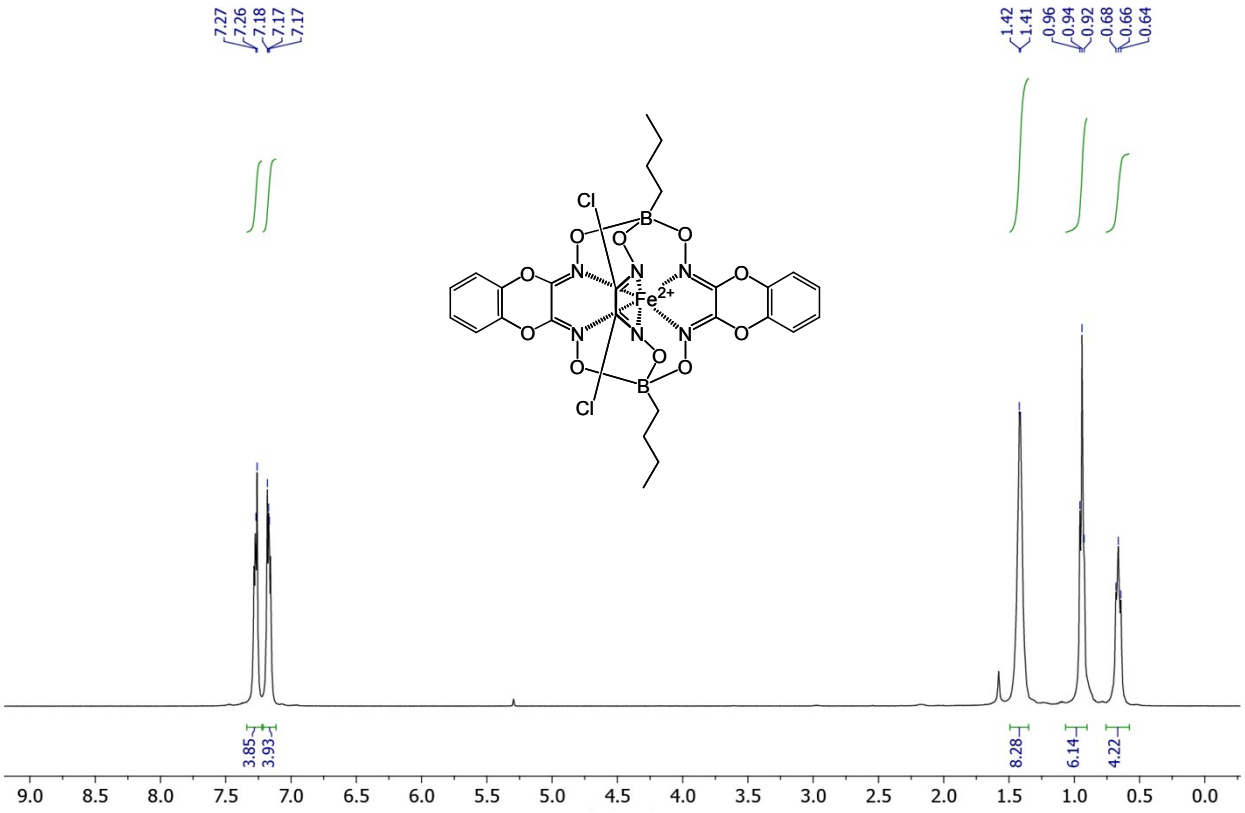

Figure S13. ^{1}H NMR spectrum for the $CDCl_3$ solution of the clathrochelate $Fe(Cl_2Gm)(PrchGm)_2(B\textit{n}\text{-}C_4H_9)_2$ (**7**).

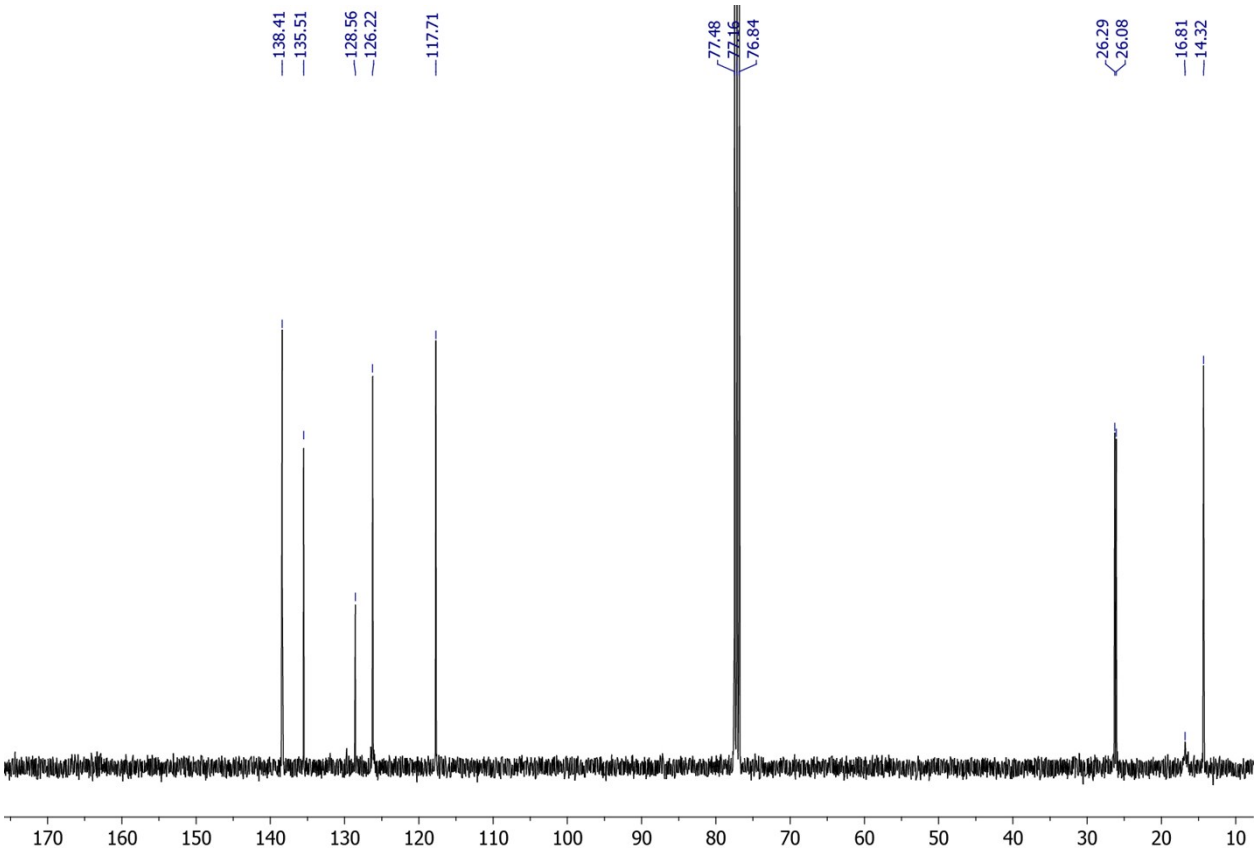

Figure S14. $^{13}C\{^{1}H\}$ NMR spectrum for the $CDCl_3$ solution of the clathrochelate $Fe(Cl_2Gm)(PrchGm)_2(B\textit{n}\text{-}C_4H_9)_2$ (**7**).

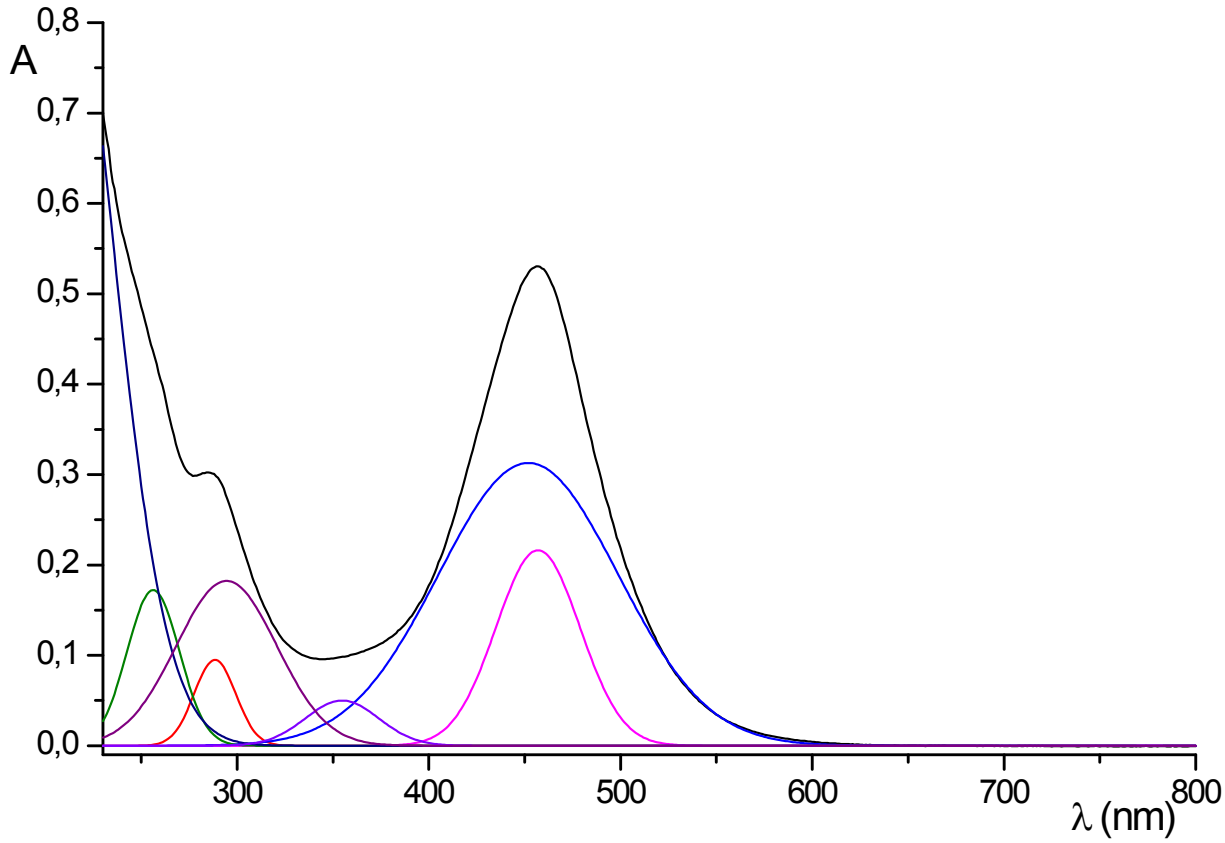

Figure S15. UV-Vis spectrum for the dichloromethane solution of the clathrochelate Fe(S_2-Nx)(Cl_2Gm)$_2$(B*n*-C_4H_9)$_2$ (**1**) and its deconvolution on the Gaussian components.

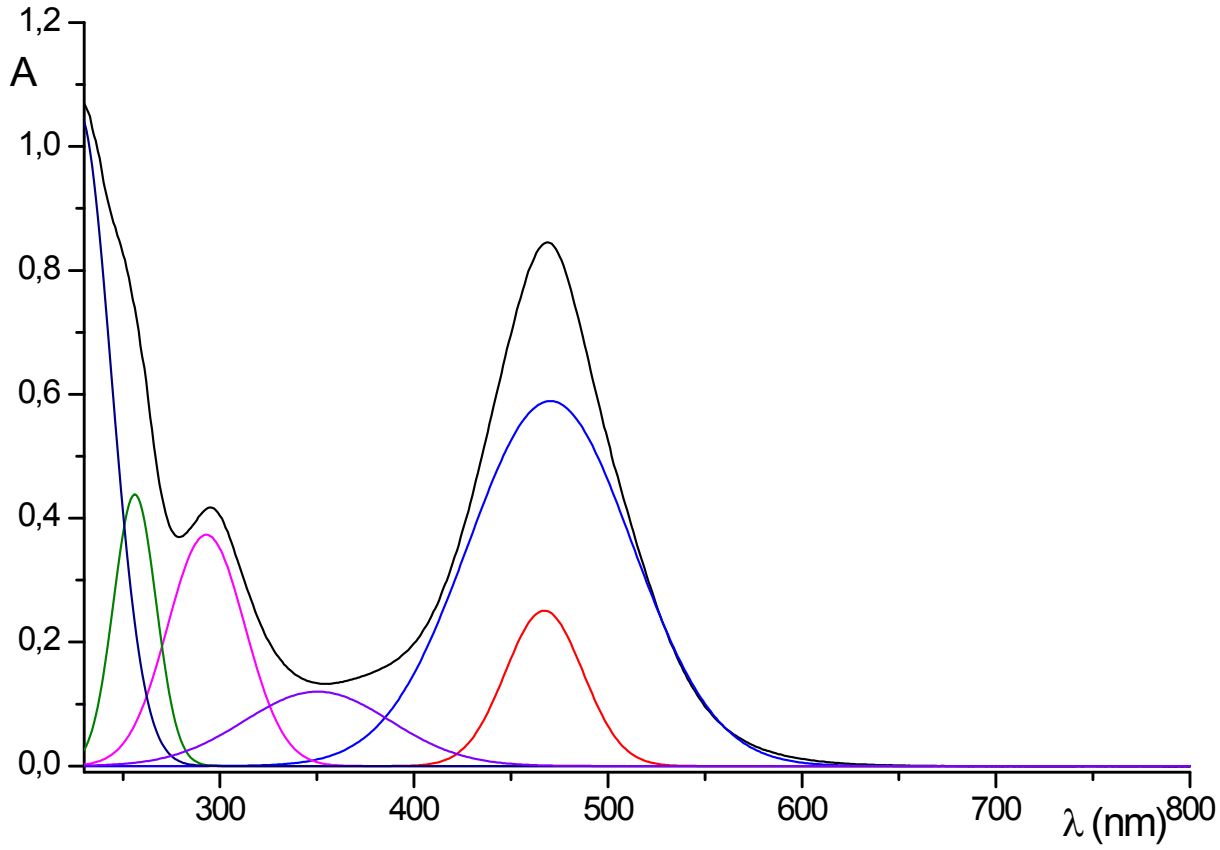

Figure S16. UV-Vis spectrum for the dichloromethane solution of the clathrochelate Fe(S_2-Nx)$_2$(Cl_2Gm)(B*n*-C_4H_9)$_2$ (**2**) and its deconvolution on the Gaussian components.

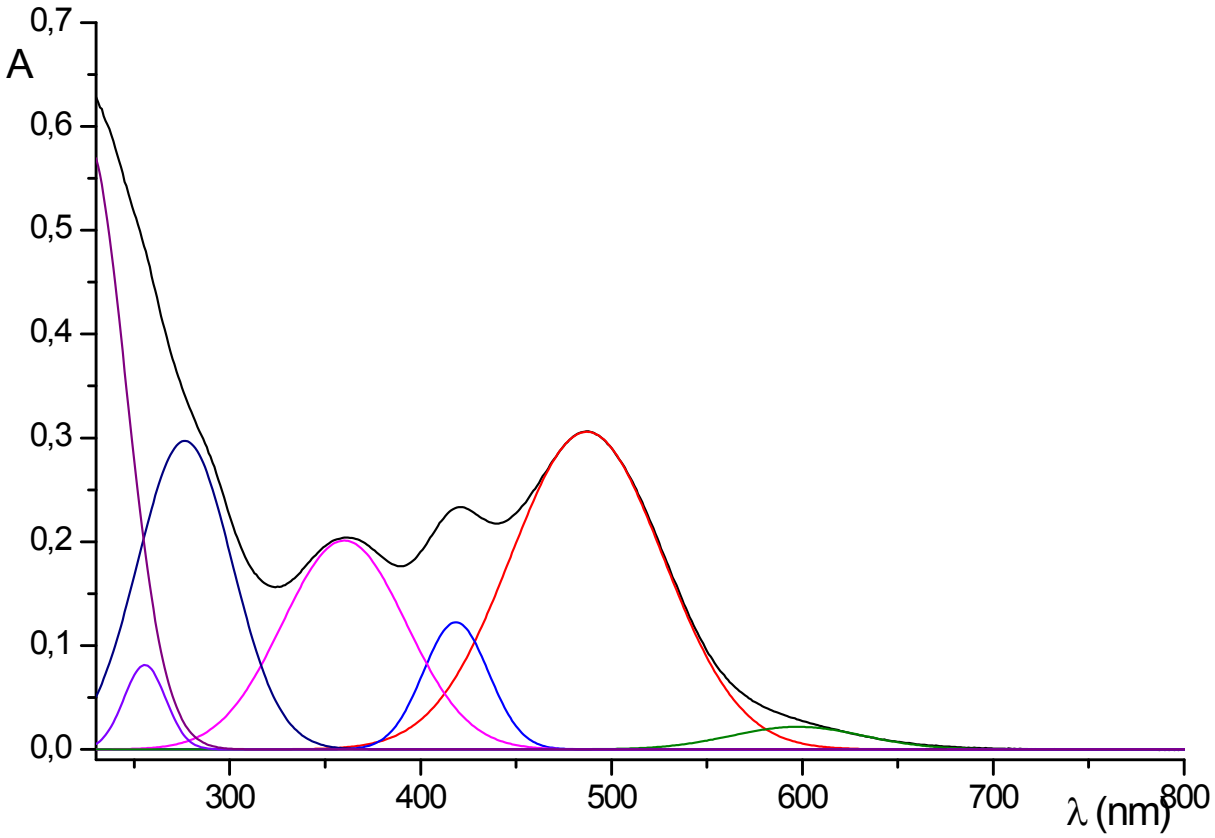

Figure S17. UV-Vis spectrum for the dichloromethane solution of the clathrochelate Fe(N_2-Nx)(Cl_2Gm)$_2$(B*n*-C_4H_9)$_2$ (**3**) and its deconvolution on the Gaussian components.

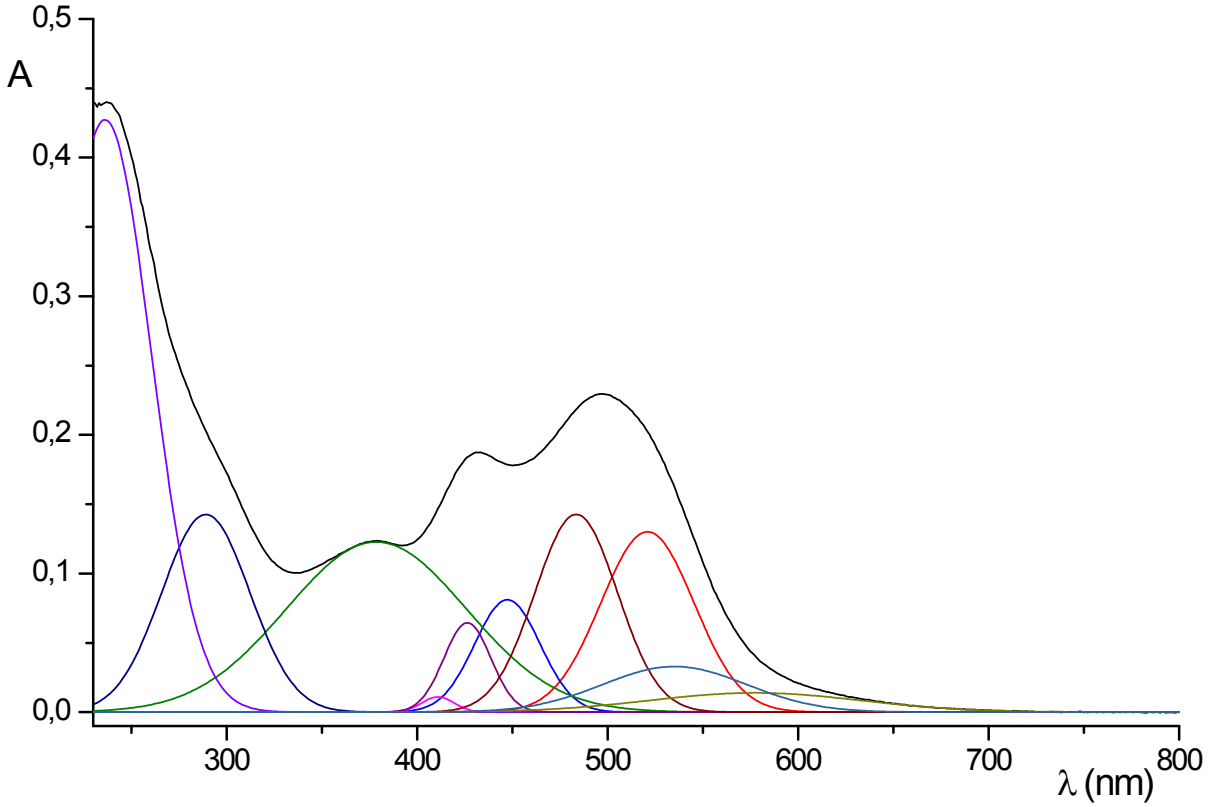

Figure S18. UV-Vis spectrum for the dichloromethane solution of the clathrochelate Fe(N_2-Nx)(S_2-Nx)(Cl_2Gm)(B*n*-C_4H_9)$_2$ (**4**) and its deconvolution on the Gaussian components.

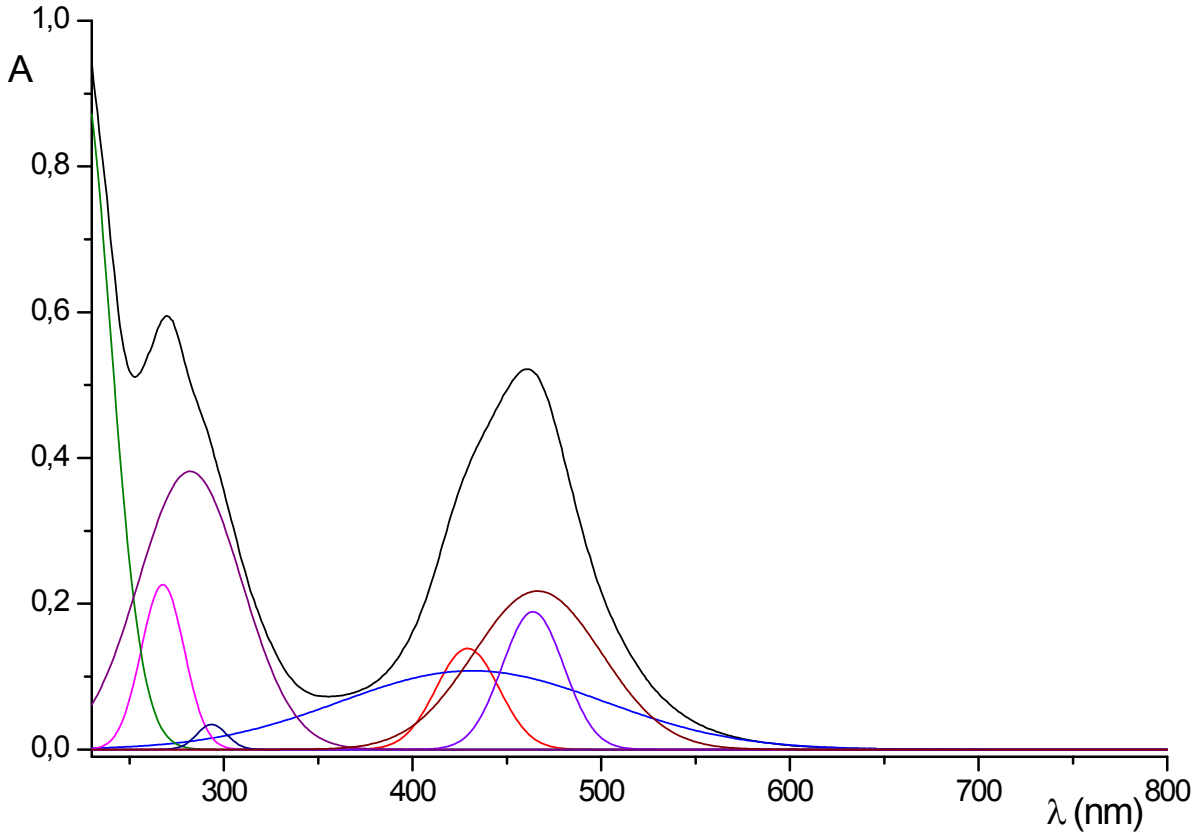

Figure S19. UV-Vis spectrum for the dichloromethane solution of the clathrochelate $Fe(PrchGm)_3(B\textit{n}\text{-}C_4H_9)_2$ (**5**) and its deconvolution on the Gaussian components.

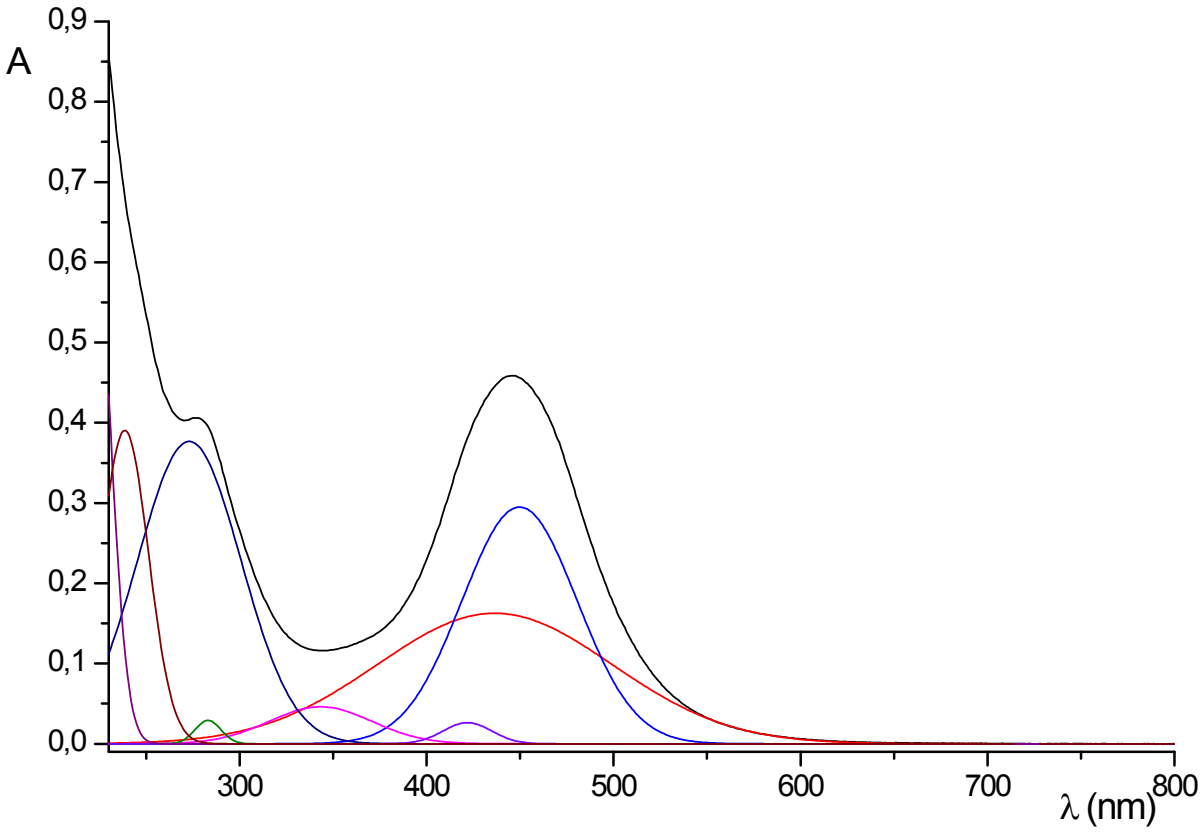

Figure S20. UV-Vis spectrum for the dichloromethane solution of the clathrochelate $Fe(Cl_2Gm)_2(PrchGm)(B\textit{n}\text{-}C_4H_9)_2$ (**6**) and its deconvolution on the Gaussian components.

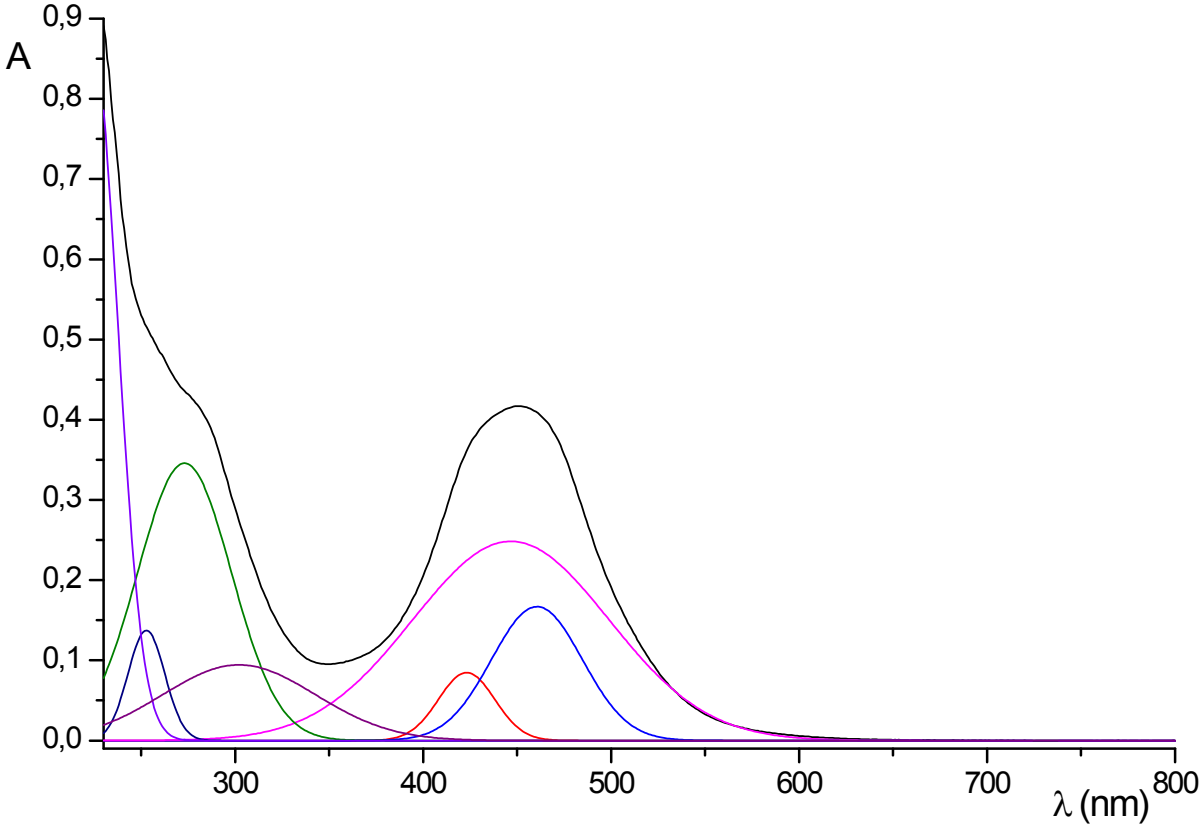

Figure S21. UV-Vis spectrum for the dichloromethane solution of the clathrochelate $Fe(Cl_2Gm)(PrchGm)_2(B\textit{n}\text{-}C_4H_9)_2$ (**7**) and its deconvolution on the Gaussian components.

Table S1. Crystallographic data and refinement parameters for the crystals **Fe(Cl$_2$Gm)$_2$(*N$_2$*-Nx)(B*n*-C$_4$H$_9$)$_2$**, **1.5 Fe(*S$_2$*-Nx)$_2$(Cl$_2$Gm)(B*n*-C$_4$H$_9$)$_2$ · 0.5 Fe(*S$_2$*-Nx)$_3$(B*n*-C$_4$H$_9$)$_2$** and **Fe(PrchGm)$_3$(B*n*-C$_4$H$_9$)$_2$**

	Fe(Cl$_2$Gm)$_2$(*N$_2$*-Nx)(B*n*-C$_4$H$_9$)$_2$	**1.5 Fe(*S$_2$*-Nx)$_2$(Cl$_2$Gm)(B*n*-C$_4$H$_9$)$_2$ · 0.5 Fe(*S$_2$*-Nx)$_3$(B*n*-C$_4$H$_9$)$_2$**	**Fe(PrchGm)$_3$(B*n*-C$_4$H$_9$)$_2$**
Empirical formula	$C_{16}H_{23}B_2Cl_4FeN_8O_6$	$C_{37}H_{54}B_4Cl_3Fe_2N_{12}O_{12}S_9$	$C_{32}H_{30}B_2Fe\ N_6O_{12}$
Fw	642.69	1408.75	768.09
T, K	120	120	120
Crystal system	monoclinic	triclinic	tetragonal
Space group	*P 2$_1$/c*	$P\,\bar{1}$	*P 4$_1$ 2$_1$ 2*
Z	4	2	4
a, Å	9.453(2)	14.4860(4)	11.0772(2)
b, Å	12.533(3)	15.3721(3)	11.0772(2)
c, Å	23.913(5)	15.7873(4)	26.6909(9)
α, °	90	117.4170(10)	90.00
β, °	115.700(4)	99.084(2)	90.00
γ, °	90	107.0350(10)	90.00
V, Å^3	2552.9(10)	2800.58(12)	3275.09(14)
d_{calc} (g·cm^{-3})	1.672	1.671	1.558
μ (mm^{-1})	1.060	91.91	5.37
F(000)	6300	1446	1584
2θ$_{max}$, °	58	135	52
Measured refl.	29746	35554	29809
Independent reflections (R$_{int}$)	7798 (0.080)	9471 (0.045)	4981 (0.037)
Obs.refl./restraints/ parameters	5315 / 24 / 353	7854 / 14 / 720	4529 / 0 / 241
R,[a] % [I > 2σ(I)]	0.114	0.0506	0.0300
R_w,[b] %	0.255	0.1043	0.0772
GOF[c]	1.06	0.99	1.01
Residual electron density, eÅ^{-3}(d$_{min}$/d$_{max}$)	1.013 / -1.056	1.005/-0.932	0.430/-0.437

[a] $R = \Sigma\,\big|\,|F_o| - |F_c|\,\big| / \Sigma\,|F_o|$. [b] $R_w = [\Sigma(w(F_o^2 - F_c^2)^2)/\Sigma(w(F_o^2))]^{1/2}$. [c] GOF = $[\Sigma w(F_o^2 - F_c^2)^2/(N_{obs} - N_{param})]^{1/2}$

Table S2. UV-vis spectra (λ_{max}/nm, $\varepsilon \cdot 10^{-3}$ $mol^{-1}Lcm^3$) for the triribed-functionalized iron(II) clathrochelates

Compound	λ_1	λ_2	λ_3	λ_4	λ_5	λ_6	λ_7	λ_8	λ_9	λ_{10}	λ_{11}
Fe(*S*$_2$-Nx)(Cl$_2$Gm)$_2$(B*n*-C$_4$H$_9$)$_2$	256(5.5)	288(3.0)	294(5.8)	355(1.6)			452(10)	457(6.9)			
Fe(*S*$_2$-Nx)$_2$(Cl$_2$Gm)(B*n*-C$_4$H$_9$)$_2$	256(13)		293(11)	350(3.6)			467(7.5)	470(18)			
Fe(*N*$_2$-Nx)(Cl$_2$Gm)$_2$(B*n*-C$_4$H$_9$)$_2$	256(2.7)		277(10)	360(6.7)			487(10)				597(0.7)
Fe(*N*$_2$-Nx)(*S*$_2$-Nx)(Cl$_2$Gm)(B*n*-C$_4$H$_9$)$_2$	236(13)	289(4.2)		378(3.6)	411(0.3)	426(1.9)	447(2.4)	484(4.2)	521(3.8)	535(1.0)	577(0.4)
Fe(PrchGm)$_3$(B*n*-C$_4$H$_9$)$_2$	268(7.2)	282(12)	294(1.1)			429(4.4)	432(3.5)	464(6.0)	466(6.9)		
Fe(Cl$_2$Gm)$_2$(PrchGm)(B*n*-C$_4$H$_9$)$_2$	239(13)	273(13)	283(1.0)	343(1.5)		422(0.9)	436(5.4)	450(9.8)			
Fe(Cl$_2$Gm)(PrchGm)$_2$(B*n*-C$_4$H$_9$)$_2$	253(5.4)	273(13)	302(3.7)			423(3.3)	447(9.6)	461(6.5)			
Fe(Cl$_2$Gm)$_3$(B*n*-C$_4$H$_9$)$_2$ [17]		259(7.9)	285(5.4)	313(2.7)			423(4.8)	453 (15)			